The Sigma-Delta CNN with Second Order Noise Shaping Property

Masatake Hirano*, Hisashi Aomori*, Tsuyoshi Otake† and Mamoru Tanaka*
*Sophia University
Department of Electrical and Electronics Engineering
7-1 Kioi-cho, Chiyoda-ku, Tokyo
†Tamagawa University
Department of Software Science
6-1-1 Tamagawagakuen, Machida-shi, Tokyo
JAPAN
tottipanty@gmail.com, aomori@ieee.org, otake@ieee.org, Mamoru.Tanaka@gmail.com

Abstract: In this paper, a novel spatial domain 2-D sigma-delta modulation using two-layered discrete-time cellular neural networks (DT-CNNs) with multi-stage noise shaping (MASH) property is proposed. Although the sigma-delta modulation is widely used for realizing of analog to digital converter (ADC), sigma-delta concepts are only for 1-D signals. Signal processing in the digital domain is extremely useful in 2-D signals such as image processing, medical imaging, ultrasound imaging and so on. In the proposed architecture, the A-template is used for a digital to analog converter (DAC), the C-template works as an integrator, and the nonlinear output function is used for the bilevel output. Besides, due to the CNN characteristic, each pixel of an image corresponds to the cell of CNN, and each cell is connected spatially by the A-template. Also, the multi stage noise shaping (MUSH) property, which is one of a very effective framework for a high order sigma-delta modulation, is exploited for realizing a second order sigma-delta modulator by cascade connected first-order CNN sigma-delta modulators.

Key–Words: Celluler neural network, Sigma-delta modulation, Image reconstruction, Image halftoning, Second-order noise shaping.

1 Introduction

The sigma-delta modulation [1] is a widely used and well-known technique for converting analog signals into pulse digital sequences. One significant advantage of this method is that the analog signals are converted using only a 1-bit analog to digital converter (ADC). Therefore, the precision of analog signal processing circuits is usually much less than the resolution of the overall converter [2] – [5]. The important characteristics of sigma-delta modulation are signal reconstruction and noise shaping properties. In the sigma-delta modulation, quantization noises are distributed into the high frequency regions by the noise shaping property with an oversampling technique. Also, the original input analog signal is reconstructed by the collective operation of low-pass decimation filtering of a 1-bit digital data stream which is the output of a low-resolution quantizer incorporated within a feed back loop. However, the original sigma-delta modulation technique is limited to 1-D signals.

The multi stage noise shaping (MASH) [6] is a very effective concept for constructing a high-order sigma-delta modulator by combination of basic first-order sigma-delta modulators. This paper uses the characteristic of the MASH modulator for the 2-D sigma-delta modulation. The basic characteristics of MASH are that quantization noise in the first sigma-delta loop is requantized by the next sigma-delta loop and cancelled by adding the requantized noise to the first stage signal. Therefore, the 2-D sigma-delta modulator with MASH property can reduce the quantization noise more than the 1-D sigma-delta modulator.

The cellular neural networks (CNNs) [7] has been applied to many signal processing applications such as image compression, filtering, nonlinear phenomena, retinal imaging and pattern recognition [8] – [15]. The image processing tasks using CNNs were mainly developed for black and white output images, since a cell in the CNN has a stable equilibrium point at the two saturation regions of the piecewise linear output function after the transient has decayed toward equilibrium [16] [17]. The output at the two saturation regions corresponds to the black and white pixels. In contrast, the nonlinear dynamics of a CNN with a two-level output function converts the input images into bilevel pulse digital sequences. Actually, CNN can convert the multi-bit image into an optimal binary halftone image. This significant characteristic of a CNN suggests the possibility of a spatial domain sigma-delta modulation. The nonlinear dynamics by feed back A-template is one of the significant characteristics of CNNs. This paper proposes a novel second-order spatial domain sigma-delta modulator by cascaded CNN sigma-delta modulators [18] – [20]. Because of the MASH property, this method can be composed using two basic first-order CNN sigma-delta modulators. Moreover, stability conditions of the proposed CNN system can be described by that of the conventional CNN having C-template.

2 First-order CNN Σ Δ Modulator

2.1 CNN Design

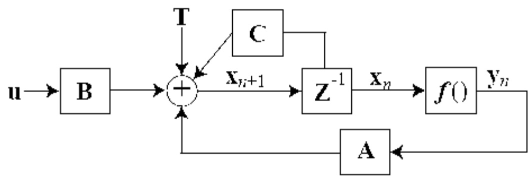

Figure 1: The block diagram of the DT-CNN: z^{-1} is a time-delay element.

To derive a DT-CNN with a C-template, we consider the continuous-time cellular neural network (CT-CNN). The state equation of a CT-CNN is given by

$$C\frac{dx_{ij}(t)}{dt} = -\frac{1}{R_x}x_{ij}(t) + \sum_{C(k,l)\in N_r(i,j)} A(i,j;k,l)y_{kl}(t) + \sum_{C(k,l)\in N_r(i,j)} B(i,j;k,l)u_{kl} + T_h, \quad (1)$$

where C, R_x, $x_{ij}(t)$, $y_{ij}(t)$, $u_{ij}(t)$, T_h and $N_r(i,j)$ are the linear capacitor, the linear resistor, the state variable, the output, the input, the threshold, and the $r-$neighborhood of the cell $C(i,j)$ as $N_r(i,j) = \{C(k,l)|\max\{|k-i|,|l-j|\} \le r\}$, respectively. $A(i,j;k,l)$ and $B(i,j;k,l)$ are feed back and feed forward template coefficients. The discrete version of (1) is described as

$$C\frac{x_{ij}(t+\Delta t)-x_{ij}(t)}{\Delta t} = -\frac{1}{R_x}x_{ij}(t) + \sum_{C(k,l)\in N_r(i,j)} A(i,j;k,l)y_{kl}(t) + \sum_{C(k,l)\in N_r(i,j)} B(i,j;k,l)u_{kl} + T_h. \quad (2)$$

Let $C = 1$ and $\Delta t = 1$, then we have

$$x_{ij}(t+1) = \left(1-\frac{1}{R_x}\right)x_{ij}(t) + \sum_{C(k,l)\in N_r(i,j)} A(i,j;k,l)y_{kl}(t) + \sum_{C(k,l)\in N_r(i,j)} B(i,j;k,l)u_{kl} + T_h. \quad (3)$$

In the case of $R_x = 1$, the DT-CNN proposed by Harrer and Nossek can be derived. The state equation of the DT-CNN is described as

$$x_{ij}(t+1) = \sum_{C(k,l)\in N_r(i,j)} C(i,j;k,l)x_{kl}(t) + \sum_{C(k,l)\in N_r(i,j)} A(i,j;k,l)y_{kl}(t) + \sum_{C(k,l)\in N_r(i,j)} B(i,j;k,l)u_{kl} + T_h, \quad (4)$$

$$y(t) = f(x(t)), \quad (5)$$

$$f(x) = \begin{cases} 1 & x \ge 1, \\ \hat{f}(x) & |x| \le 1, \\ -1 & x \le -1, \end{cases} \quad (6)$$

where $C(i,j;k,l)$ is the neighborhood connection coefficients between state variables. The coefficients of a C-template are defined by

$$C(i,j;k,l) = \mathrm{diag}\{\xi, \cdots, \xi\}, \quad (7)$$

$$\xi = 1 - \frac{1}{R_x}. \quad (8)$$

Then the state equation can be rewritten as

$$x_{ij}(t+1) = \xi x_{ij}(t) + \sum_{C(k,l)\in N_r(i,j)} A(i,j;k,l)y_{kl}(t) + \sum_{C(k,l)\in N_r(i,j)} B(i,j;k,l)u_{kl} + T_h. \quad (9)$$

Also, the energy function $E(t)$ can be defined by

$$E(t) = -\frac{1}{2}\sum_{(i,j)}\sum_{(k,l)} A(i,j;k,l)y_{ij}(t)y_{kl}(t) - \sum_{(i,j)}\sum_{(k,l)} B(i,j;k,l)y_{ij}(t)u_{kl} - \sum_{(i,j)} T_h y_{ij}(t) + (1-\xi)\sum_{(i,j)}\int_0^{y_{ij}(t)} f^{-1}(y)dy, \quad (10)$$

where $f^{-1}(\cdot)$ is the pseudo-inverse function of $f(\cdot)$ defined as

$$f^{-1}(y) = \begin{cases} 1 & y = 1, \\ \hat{f}^{-1}(y) = x & |y| < 1, \\ -1 & y = -1. \end{cases} \quad (11)$$

The following theorem holds in terms of the Lyapunov function [18].

Theorem 1 *If $A(i, j; k, l) = A(k, l; i, j)$, then the energy function $E(t)$ is monotonously decreasing.*

Since the energy function $E(t)$ does not calculate exactly, the present form of the energy function cannot be applied to various nonlinear optimization problems. Therefore, let

$$\sum_{(i,j)} \int_0^{y_{ij}(t)} f^{-1}(y)dy \approx \frac{1}{2} y_{ij}(t)^2, \tag{12}$$

and then the approximated Lyapunov energy function is obtained in matrix form as

$$E(t) = -\frac{1}{2}\boldsymbol{y}^T (\boldsymbol{A} - (1-\xi)\boldsymbol{I})\, \boldsymbol{y} - \boldsymbol{y}^T \boldsymbol{Bu} - \boldsymbol{T}_{\boldsymbol{h}}^T \boldsymbol{y}, \tag{13}$$

where $\boldsymbol{a}^T$ is the transposed matrix of $\boldsymbol{a}$. Moreover, the steady-state behavior of a CNN was discussed in [21], and the following theorem was proven.

Theorem 2 *If the center of the A-template of a CNN satisfies*

$$A(i, j; i, j) > \frac{1}{R_x}, \tag{14}$$

then each cell of the CNN settles at the stable equilibrium points after the convergence of the dynamics.

If $f(\cdot)$ corresponds to the unit quantization function (1-bit quantizer), then the integration term of the Lyapunov energy function can be approximated by

$$\sum_{(i,j)} \int_0^{y_{ij}(t)} f^{-1}(y)dy \approx 0. \tag{15}$$

Therefore, (20) can be rewritten as

$$E(t) = -\frac{1}{2}\boldsymbol{y}^T \boldsymbol{Ay} - \boldsymbol{y}^T \boldsymbol{Bu} - \boldsymbol{T}_{\boldsymbol{h}}^T \boldsymbol{y}. \tag{16}$$

In addition, the stability condition for the center element of the A-template can be given by

$$A(i, j; i, j) > 0. \tag{17}$$

Fig. 1 shows the block diagram of the DT-CNN. The state equation of the DT-CNN is described in matrix form as

$$\boldsymbol{x_{n+1}} = \boldsymbol{Af(x_n)} + \boldsymbol{Bu} + \boldsymbol{T_h}, \tag{18}$$

$$\boldsymbol{y_{n+1}} = \boldsymbol{f(x_{n+1})}, \tag{19}$$

where $\boldsymbol{u}$ is the input matrix, $\boldsymbol{x}$ is the state variable and $\boldsymbol{f}()$ is the multi-level quantizing function. $\boldsymbol{A}$ and $\boldsymbol{B}$ are feed back and feed forward template coefficients and $\boldsymbol{T_h}$ is the threshold, respectively. The Lyapunov energy function is obtained in matrix form as

$$\mathrm{E} = -\frac{1}{2}\boldsymbol{y}^T \boldsymbol{Ay} - \boldsymbol{y^T Bu} - \boldsymbol{T_h}^{\boldsymbol{T}} \boldsymbol{y}. \tag{20}$$

For achieving a spatial domain 2-D sigma-delta modulation by DT-CNN, CNN templates and parameter which satisfy a nonlinear optimization problem minimizing the distortion between the input image and the output image including quantization noises, should be designed.

In the CNN dynamics, the objective function must provide the optimal halftoning image from the coefficients including noises. Also, the difference between the output halftoning image and the input image should be small. Hence, the objective function called distortion function is given by

$$\mathrm{dist}(\boldsymbol{y}, \boldsymbol{u}) = \left\| \frac{1}{2}\boldsymbol{y}^T (\boldsymbol{Gy} - \boldsymbol{u}) \right\|, \tag{21}$$

where $\boldsymbol{G}$ is a Gaussian filter.

Since the reconstruction image is obtained by the summation of bilevel pulse sequence images, the quality of the reconstruction image can be determined like MSE:

$$\mathrm{err}(\boldsymbol{y}, \boldsymbol{u}) = \left\| \boldsymbol{u} - \boldsymbol{G} \sum_t \boldsymbol{y}(t) \right\|. \tag{22}$$

Although we can get three conditions which determine the spatial domain 2-D sigma-delta modulation, (22) can not be applied directly to the DT-CNN due to the summation term. It can be said that the reconstruction image is gradually improved because of the Lyapunov energy function property. Therefore the output that minimizes (21) becomes a solution which minimizes (22). In other words, the DT-CNN parameter for image binarization can be obtained from two conditions.

2.2 CNN Templates and Parameters

By the comparison between (20) and (21), the $\boldsymbol{A}$, $\boldsymbol{B}$, and $\boldsymbol{C}$ templates and the parameter $\boldsymbol{T}_h$ of the first layer DT-CNN for image halftoning can be determined as

$$\begin{aligned} \boldsymbol{A} &= A(i, j; k, l), \qquad C(k, l) \in N_r(i, j) \qquad (23) \\ &= -\frac{1}{2\pi\sigma^2} \exp\left(-\frac{(k-i)^2 + (l-j)^2}{2\sigma^2}\right), \end{aligned}$$

$$\begin{aligned} \boldsymbol{B} =& B(i,j;k,l), \qquad C(k,l) \in N_r(i,j) \\ =& \begin{cases} 1 & \text{if } k = i \text{ and } l = j\ , \\ 0 & \text{otherwise,} \end{cases} \end{aligned} \tag{24}$$

$$\begin{aligned} \boldsymbol{C} =& C(i,j;k,l), \qquad C(k,l) \in N_r(i,j) \\ =& \begin{cases} \xi & \text{if } k = i \text{ and } l = j\ , \\ 0 & \text{otherwise,} \end{cases} \end{aligned} \tag{25}$$

$$\boldsymbol{T}_h = \boldsymbol{O}, \tag{26}$$

where σ is the standard deviation of the Gaussian function, and $\boldsymbol{O}$ is a zero matrix. Then we can recall the dynamics using the above parameters as follows;

$$x(t+1) = \xi x(t) + \sum_{C(k,l)\in N_r(i,j)} A(i,j;k,l) y_{kl}(t) + u_{ij}, \tag{27}$$

$$y(t) = f(x(t)), \tag{28}$$

$$f(x) = \begin{cases} 1 & x \geq 0, \\ -1 & x < 0. \end{cases} \tag{29}$$

The output function $f(\cdot)$ corresponds to the 1-bit quantizer.

The output of the first layer DT-CNN $\hat{\boldsymbol{y}}$ becomes the input of the second layer DT-CNN for image reconstruction. Obviously, the output of the first layer DT-CNN can minimize (22). Hence, the reconstruction image $\tilde{\boldsymbol{y}}$ is given by

$$\tilde{y}_{ij} = \sum_{y_{kl}\in N_r(i,j)} \hat{B}(i,j;k,l) \hat{y}_{ij}, \tag{30}$$

where

$$\begin{aligned} \hat{B} =& \hat{B}(i,j;k,l), \qquad C(k,l) \in N_r(i,j) \\ =& \frac{1}{2\pi\sigma^2} \exp\left(-\frac{(k-i)^2 + (l-j)^2}{2\sigma^2} \right). \end{aligned} \tag{31}$$

3 Proposed Second-Order Σ Δ CNN

3.1 System

The proposed second-order sigma-delta modulator by DT-CNN is shown in Fig. 2. It is composed of the cascade connected two first-order CNN sigma-delta modulators. Therefore, the system is an equivalent framework of the spatial domain second-order sigma-delta modulator with MASH property.

In the 1st Layer DT-CNN, the input signal is quantized. The 2-D distributed quantization noises given by the 1st Layer DT-CNN1 become an input

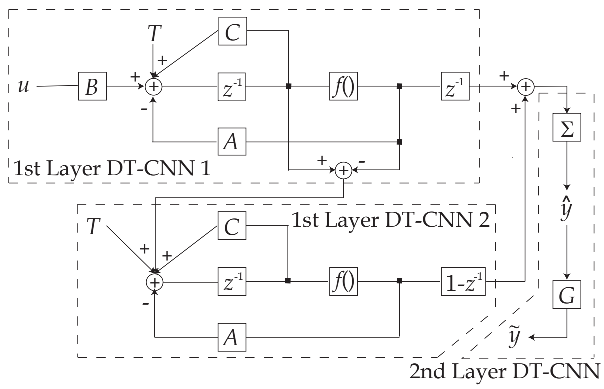

Figure 2: Two-layered second-order sigma-delta modulator using a cascaded DT-CNN: In the first layer DT-CNN, the first stage in the part enclosed with the dotted line was named "1st Layer DT-CNN1", and the second stage was named "1st Layer DT-CNN2". In the second layer DT-CNN, the part enclosed with the dotted line was named "2nd Layer DT-CNN".

to the second stage, and they are remodulated by the 1st Layer DT-CNN2. In addition, the 2-D remodulated quantization noises by the 1st Layer DT-CNN2 are added to the output by the 1st Layer DT-CNN1, and total quantization noises through the modulation can be reduced. Therefore, the good binary halftoning images are provided by the 2-D sigma-delta modulator using DT-CNN at each iteration of dynamics.

In the 2nd layer DT-CNN, the output by the 1st layer DT-CNN1 and DT-CNN2 are the input of the 2nd layer DT-CNN. In the 2nd layer DT-CNN which has no dynamics, bilevel pulse digital sequence images are added for the reconstruction image. After the transient of the dynamics of the 1st layer DT-CNN, the optimal reconstruction image is obtained. According as the sigma-delta characteristic, the reconstruction image gradually approaches the original image by the iteration of dynamics.

3.2 Noise Shapong Property

In the Z-domain, the first layer and the second layer of the proposed architecture is shown in Fig. 3. The input and output relationship is given by

$$\begin{aligned} Y_1(z_v, z_h) =& U(z_v, z_h) \frac{z_t^{-1}}{1 - \xi z_t^{-1}} \\ & - A(z_v, z_h) Y_1(z_v, z_h) \frac{z_t^{-1}}{1 - \xi z_t^{-1}} \\ & + N_1(z_v, z_h), \end{aligned} \tag{32}$$

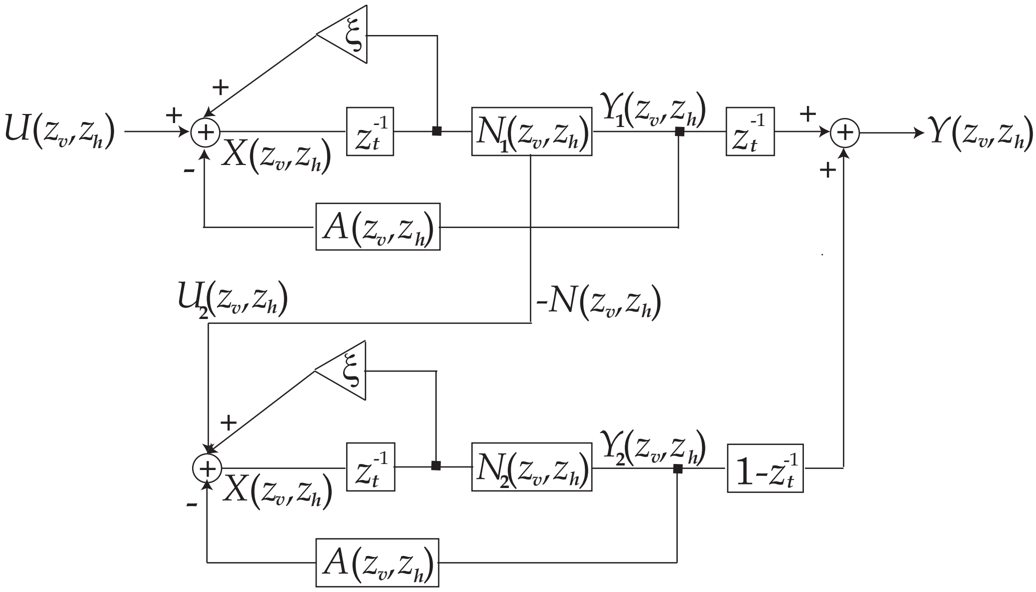

Figure 3: The first layer DT-CNN in Z-domain.

where z_v is the vertical frequency, z_h is the horizontal frequency and z_t^{-1} is a time-delay element. $U(z_v, z_h)$, $Y_1(z_v, z_h)$ and $N(z_v, z_h)$ are the 2-D Z-transform of the input, the output and the 1-bit quantizer, respectively.

If the DAC with the A-template is ideal, then (32) can be rewritten as

$$Y_1(z_v, z_h) = \frac{z_t^{-1}}{1+(1-\xi)z_t^{-1}} U(z_v, z_h) + \frac{1-\xi z_t^{-1}}{1+(1-\xi)z_t^{-1}} N_1(z_v, z_h). \tag{33}$$

If ξ is a small value, (33) can be approximated by

$$Y_1(z_v, z_h) \approx z_t^{-1} U(z_v, z_h) + \left(1 - z_t^{-1}\right) N_1(z_v, z_h). \tag{34}$$

In the same maner, the input and output relationship of the 1st layar DT-CNN2 is calculated when the input of the 1st layar DT-CNN2 is assumed to $\boldsymbol{U_2(z_v, z_h)}$. The input and output relationship of the 1st layar DT-CNN2 is given by

$$Y_2(z_v, z_h) \approx z_t^{-1} U_2(z_v, z_h) + \left(1 - z_t^{-1}\right) N_2(z_v, z_h). \tag{35}$$

Therefore, the total output $\boldsymbol{Y(z_v, z_h)}$ is

$$\begin{aligned} Y(z_v, z_h) &= z_t^{-1} Y_1(z_v, z_h) + \left(1 - z_t^{-1}\right) Y_2(z_v, z_h) \\ &= z_t^{-2} U(z_v, z_h) + \left(1 - z_t^{-1}\right)^2 N_2(z_v, z_h), \end{aligned} \tag{36}$$

where the input of the $\boldsymbol{U_2(z_v, z_h)}$ is $\boldsymbol{-N(z_v, z_h)}$ of the input from the first layer. (36) shows the second-order noise shaping property.

4 Experimental Results

In order to evaluate the performance of our proposed the second-order sigma-delta modulator using two-layered DT-CNN, we implemented the A/D system by ANSI C++. We applied our system to the 8-bit standard gray-scale test images; "Aerial," "Barbara," "Boat," "Couple," "Crowd," "Goldhill," "Lena," and "Milkdrop." The size of all the images is 512×512 pixels. Fig. 4 shows the relationship between the iteration of dynamics and the peak signal-to-noise ratio (PSNR) of the reconstructed images. These results suggest that the relevant conditions for the maximum iteration is given by $n_{max} \geq 128$.

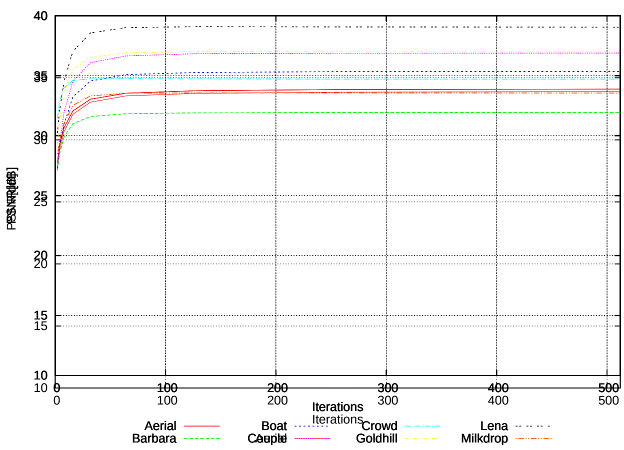

Figure 4: The relationship between iteration of dynamics and PSNR of reconstruction images.

Table 1: Optimum σ of Gaussian function and reconstruction performance in terms of PSNR (dB).

Image	Method	σ_1/σ_2/Threshold	PSNR
Aerial	Proposed	0.72	**33.75**
	1st-order	0.705	33.70
	fastiht2	127	25.58
Barbara	Proposed	0.71	**31.91**
	1st-order	0.71	31.78
	fastiht2	127	24.44
Boat	Proposed	0.77	**35.27**
	1st-order	0.755	34.45
	fastiht2	127	28.56
Couple	Proposed	0.74	**36.84**
	1st-order	0.735	36.20
	fastiht2	127	28.15
Crowd	Proposed	0.99	**34.74**
	1st-order	0.985	34.29
	fastiht2	127	29.67
Goldhill	Proposed	0.77	**37.01**
	1st-order	0.765	36.64
	fastiht2	127	29.51
Lena	Proposed	0.82	**39.09**
	1st-order	0.795	38.18
	fastiht2	127	31.35
Milkdrop	Proposed	0.74	**33.57**
	1st-order	0.74	33.32
	fastiht2	127	31.22

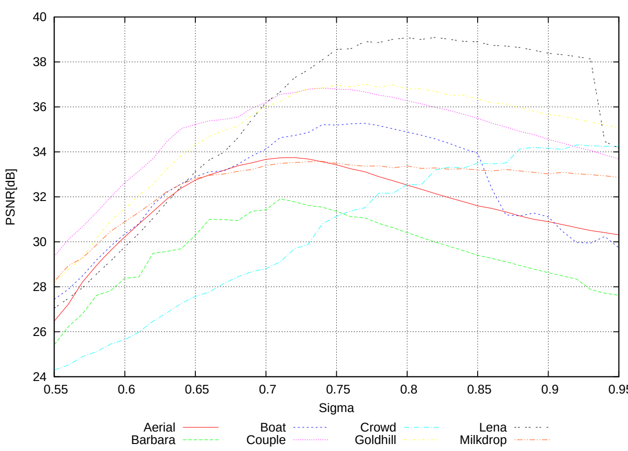

Figure 5: Reconstruction performance of each image in terms of PSNR (dB).

For the simulation, the coding factors are decided experimentally; the $r-$neighborhood of cell $r = 2$, the number of iterations $n = 128$, and the standard deviation of Gaussian σ is decided like Table 1. The reconstruction performance of the proposed method is compared with the basic first-order CNN sigma-delta modulator labeled ”1st-order” in Table 1, and the best known linear method which achieves high peak sigmal to noise ratio (PSNR) in inverse halftoning called ”fastiht2” [22], labeled ”fastiht2” in Table 1, from the Floyd-Steinberg error diffusion method [23].

Fig. 6 shows the amplitude spectrum of the Lena image. 6-(a) is the spectrum of Lena, 6-(b) is the spectrum of a denoised image with 128 iterations by the first order sigma-delta modulation, 6-(c) is the spectrum of a denoised image with 128 iterations by the second order sigma-delta modulation, 6-(d) is the spectrum of a summation image with 2 iterations by the first order sigma-delta modulation, 6-(e) is the spectrum of a summation image with 256 iterations by the first order sigma-delta modulation, 6-(f) is the spectrum of a summation image with 1024 iterations by the first order sigma-delta modulation, 6-(g) is the spectrum of a summation image with 2 iterations by the second order sigma-delta modulation, 6-(h) is the spectrum of a summation image with 256 iterations by the second order sigma-delta modulation and 6-(i) is the spectrum of a summation image with 1024 iterations by the second order sigma-delta modulation. As shown in these figures, the original signal spectrum is reconstructed and the quantization noises are shaped into high spatial frequencies by the noise shaping property. Moreover, due to the second order noise shaping property, noises of the amplitude spectrum of each iteration by the proposed algorithm are more accurmlated into high frequency regions than that of the first order. In addition, these shaped noises can be cut by the decimation filter which is provided by the 2nd layer DT-CNN.

Table 1 suggests that our proposed method has a better reconstruction performance compared with conventional methods. Fig. 5 shows the relationship of each image between σ and PSNR. Fig. 7, 8, and 9 show the input image, the modulated image and reconstruction images at each original image.

5 Conclusion

The second-order sigma-delta modulator using a cascaded sigma-delta CNNs for image reconstruction has been proposed. In our method, the nonlinear dynamics of the DT-CNN is exploited to modulate the input image. Also, the second-order sigma-delta modulator has been realized by a cascaded CNN sigma-delta

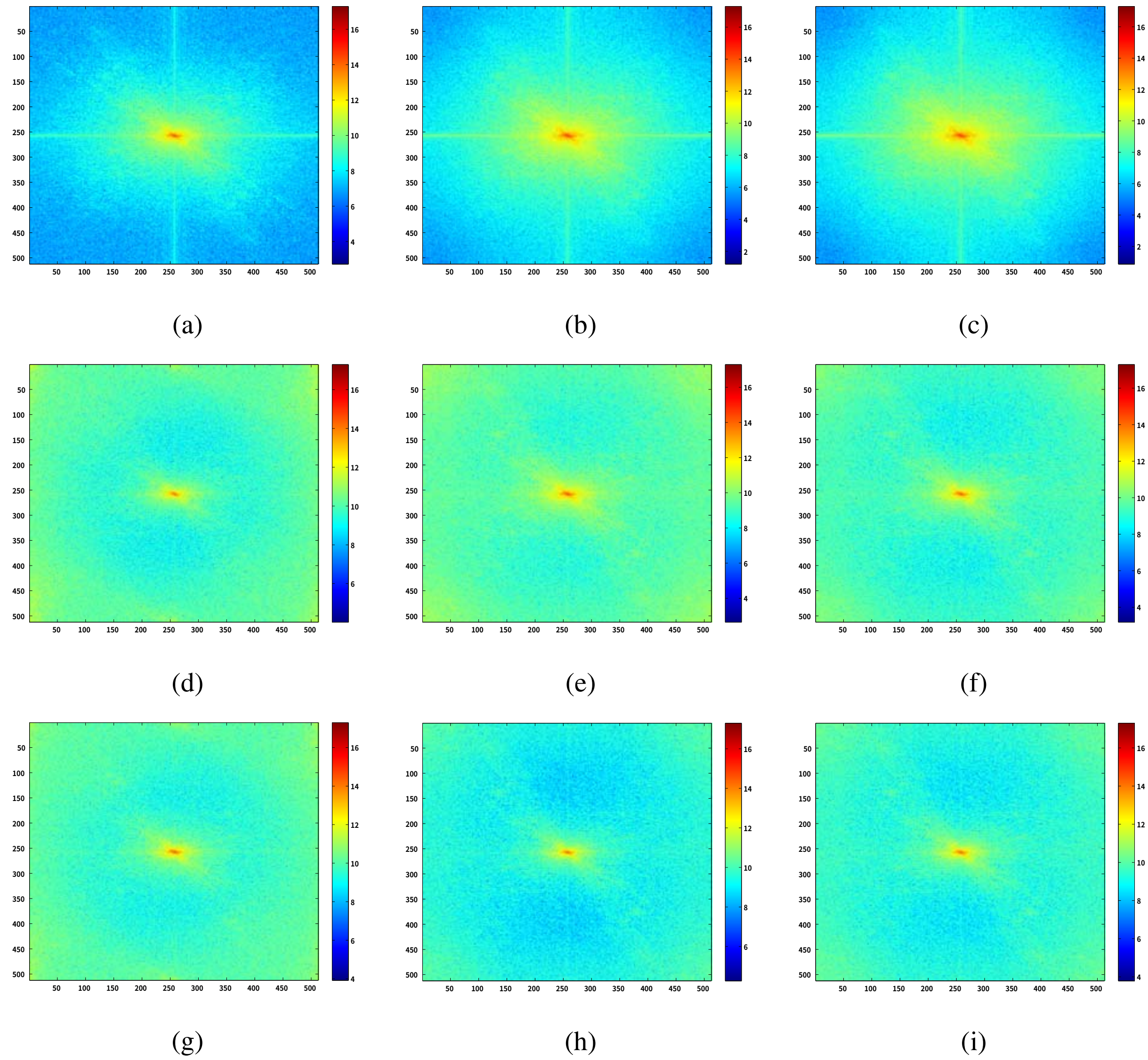

Figure 6: Amplitude spectrums of the Lena image; (a) Original Lena, (b) reconstructed image (128 iterations by the first order sigma-delta modulation), (c) reconstructed image (128 iterations by the second order sigma-delta modulation), (d) summation image (2 iterations by the first order sigma-delta modulation), (e) summation image (256 iterations by the first order sigma-delta modulation), (f) summation image (1024 iterations by the first order sigma-delta modulation), (g) summation image (2 iterations by the second order sigma-delta modulation), (h) summation image (256 iterations by the second order sigma-delta modulation), (i) summation image (1024 iterations by the second order sigma-delta modulation).

modulators.

The experimental results show that our proposed method has a better reconstruction performance compared with conventional methods. Moreover, owing to the second-order noise shaping property of the proposed system, the image reconstruction performance of the proposed method is better than that of the first-order CNN sigma-delta modulator.

Acknowledgements: This research is supported by the fund of the Open Research Center Project from MEXT of the Japanese Government (2007-2011), the fund of Grant-in-aid for young Scientists (B) from MEXT.

References:

[1] J. C. Candy and G. C. Temes, "Oversampling delta-sigma data converters: Theory, design, and simulation," IEEE Press, 1992.

Figure 7: (a) Aerial (original image), (b) Aerial (sigma-delta modulated image), (c) Aerial (denoised image), (d) Barbara (original image), (e) Barbara (sigma-delta modulated image), (f) Barbara (denoised image), (g) Boat (original image), (h) Boat (sigma-delta modulated image), (i) Boat (denoised image), (j) Couple (original image), (k) Couple (sigma-delta modulated image), (l) Couple (denoised image).

Figure 8: (a) Crowd (original image), (b) Crowd (sigma-delta modulated image), (c) Crowd (denoised image), (d) Goldhill (original image), (e) Goldhill (sigma-delta modulated image), (f) Goldhill (denoised image), (g) Lena (original image), (h) Lena (sigma-delta modulated image), (i) Lena (denoised image), (j) Milkdrop (original image), (k) Milkdrop (sigma-delta modulated image), (l) Milkdrop (denoised image).

[2] S. Hein and A. Zakhor, "On the stability of sigma delta modulators," IEEE Trans. Signal Processing, vol. 41, no. 7, pp. 2322–2348, 1993.

[3] S. C. Pinault and P. C. Lopresti, "On the behavior of the double-loop sigma-delta modulator," IEEE Trans. Circuits Syst., vol. 40, no. 8, pp. 467–479, 1993.

[4] G. C. Temes, "A 16-bit low-voltage CMOS A/D converter," IEEE Journal. Solid-State Circuit, vol. 22, no. 2, pp. 157–163, 1987.

[5] H. Wang, "A geometric view of sigma-delta modulations," IEEE Trans. Circuits Syst., vol. 39, no. 6, pp. 402–405, 1992.

[6] K. Uchimura, T. Hayashi, T. Kimura and A. Iwata, "Oversampling A-to-D and D-to-A Converters with Multistage Noise Shaping Modulators," IEEE Trans. Circuits Syst., vol. 36, no. 12, pp. 1899–1905, Des 1988.

[7] L. O. Chua and L. Yang, "Cellular neural networks: theory," IEEE Trans. Circuits Syst., vol. 35, no. 10, pp. 1257–1272, Oct. 1988.

[8] L. O. Chua and T. Roska, "The CNN paradigm," IEEE Trans. Circuits Syst., vol. 40, no. 3, pp. 147–156, 1993.

[9] H. Harrer and J. A. Nossek, "Multiple layer discrete-time cellular neural networks using time-varient templates," IEEE Trans. Circuits Syst., vol. 40, no. 3, pp. 191–199, 1993.

[10] H. Harrer and J. A. Nossek, "Some examples of preprocessing analog images with discrete-time cellular neural networks," In Proc. the 3rd IEEE intl., pp. 201–206, 1994.

[11] N. Takahashi, T. Otake and M. Tanaka, "Nonlinear interpolative effect of feedback template for image processing by discrete-time cellular neural network," Journal of Circuits Systems and Computers, vol. 12, no. 4, pp. 505–518, 2003.

[12] P. L. Venetianer and T. Roska, "Image compression by cellular neural networks," IEEE Trans. Circuits Syst., vol. 45, no. 3, pp. 205–215, 1998.

[13] R. Perfetti, E. Ricci, D. Casali and G. Constantini, "A CNN based algorithm for Retinal Vessel Segmentation," 12th WSEAS International Conference on CIRCUITS, pp. 152–157, 2008.

[14] G. K. Basnet, H. Aomori, and M. Tanaka, "Analysis of Neural Network having Nonlinear by Relaxation-based Algorithm with Fast Automatic Differentiation," WSEAS Transactions on Circuit and System, vol. 6, no.1, pp. 117–124, 2007.

[15] A. Zarandy, F. Werblin, T. Roska and L. O. Chua, "Spatial logic algorithms using basic morphological analogic CNN operations," International Journal of Circuit Theory and applications, vol. 24, no. 3, pp. 283–300, 1996.

[16] K. R. Crounse, T. Roska and L. O. Chua, "Image halftoning with cellular neural networks," IEEE Trans. Circuits Syst., vol. 40, no. 4, pp. 267–283, 1993.

[17] C. Y. Ho, D. H. Yu and S. Mori, "Synthesis of discete-time cellular neural networks for binary image processing," IEICE Trans. Fundamentals, vol. E67-A, no. 5, pp. 735–741, 1993.

[18] H. Aomori, T. Otake, N. Takahashi and M. Tanaka, "Sigma-Delta Celluler Neural Network for 2D Modulation," Neural Network, vol. 21, no. 2-3, pp. 349–357, 2008.

[19] M. Hirano, H. Aomori, T. Otake and M. Tanaka, "A Second Order Sigma-Delta Modulation by Cascaded Sigma-Delta CNNs," 12th WSEAS International Conference on CIRCUITS, pp. 86–90, 2008.

[20] H. Harrer and J. A. Nossek, "Discrete-time cellular neural networks," International Journal of Circuit Theory and applications, vol. 20, no. 5, pp. 453–467, 1992.

[21] K. Yokosawa, T. Nakaguchi, Y. Tanji and M. Tanaka, "Cellular neural networks with output function having multiple constant regions," IEEE Trans. Circuits and Systems, vol. 50, no. 7, pp. 1583–1592, 2003.

[22] T. D. Kite, N. D. Ventaka, B. L. Evans and A. C. Bovik, "High-quality inverse halftoning algorithm for error diffused halftones," IEEE Trans. Image Processing, vol. 9, pp. 1583–1592, 2000.

[23] R. Floyd and L. Steinberg, "An adaptive algorithm for spatial gray scale," In Proc. intl. symp. digest of tech. papers, society for information display, vol. 17, pp. 36–37, 1975.